A Sparsification Method for Security-Constrained Optimal Power Flow

Mohannad Alkhraijah, Devon Sigler, Bernard Knueven, Jonathan Maack

National Laboratory of the Rockies

Suggested Citation

M. Alkhraijah, D. Sigler, B. Knueven, and J. Maack, "A Sparsification Method for Security-Constrained Optimal Power Flow," in *Proceedings of the PowerUp Conference*, 2026.

BibTeX Entry

```
@inproceedings{alkhraijah2026sparsificationmethod,
  author = {Alkhraijah, Mohannad and Sigler, Devon and Knueven, Bernard and Maack,
      Jonathan},
  title = {A Sparsification Method for Security-Constrained Optimal Power Flow},
  booktitle = {Proceedings of the PowerUp Conference},
  year = {2026},
}
```

A Sparsification Method for Security-Constrained Optimal Power Flow

Mohannad Alkhraijah[†‡], Devon Sigler[†], Bernard Knueven[†], Jonathan Maack[†] .

***Abstract*—To ensure the security of power systems, operators solve security-constrained optimal power flow (SCOPF) problems to determine setpoints that satisfy operational constraints under credible contingencies. As the size of the contingency increases, the problem becomes computationally expensive, especially for very large systems with thousands of buses and lines. Solving SCOPF problems with large systems using the typical B-θ model can become intractable. Instead, a more tractable approach is to use a sensitivity-based model based on Power Transfer Distribution Factors (PTDFs). Sensitivity-based models solve SCOPF problems more efficiently when a subset of the constraints is active at optimal solutions. Although solving SCOPF with the PTDF has many advantages over the B-θ model, the PTDF matrix is very dense in real-world systems, resulting in slow computational performance. This paper presents a method for sparsifying the PTDF matrix without compromising solution quality. The proposed method is exact and yields faster computation speed. We demonstrate the proposed sparsification method on large-scale test systems representing the eastern and western interconnections of North America, with up to 78,000 buses and 10,000 contingencies. The results show that the proposed method solves the SCOPF problem 3 to 7 times faster than the common PTDF model.**

***Index Terms*—Contingency Analysis, Kron Reduction, Power Transfer Distribution Factors, Security-Constrained Optimal Power Flow**

I. Introduction

The complexity of electric power systems has been increasing over the years, driven by the high pace of electrification and growing energy demand. As the complexity of the electric power system increases, the risk and cost of outages become more significant. A major cause of large outages is related to transmission line failures [1]. To ensure the security of power systems against transmission line failures, system operators solve security-constrained optimal power flow (SCOPF) problems to find operational setpoints that ensure the security of the system under credible contingencies [2].

The complexity of SCOPF problems depends on the system size and the number of considered contingencies. Typically, SCOPF should consider all likely and low probability but high consequence contingencies [1]. However, as the number of contingencies increases, the problem can become intractable. A common approach for solving SCOPF with a large number of contingencies is to use sensitivity-based models. The advantages of using sensitivity-based approaches are prominent, especially when a few constraints are active at the optimal solution. However, using the sensitivity information produces very dense constraints, leading to slow computation when a large number of constraints are considered in the problem.

The high density of the constraints limits the number of contingencies that can be included in the SCOPF if the problem is to be solved within an acceptable time limit, i.e., real-time operations require solutions every 5–15 minutes. To overcome this challenge and increase the efficiency of sensitivity-based SCOPF problems, this paper proposes a decomposition method to sparsify the constraints matrix of SCOPF. The proposed method significantly reduces the number of non-zeros in the constraints matrix, leading to faster computational speed. Increasing computational speed will allow system operators to consider a larger number of contingencies within the optimization framework.

A. Related Work

A fundamental problem in power system operations and planning is the Optimal Power Flow (OPF). *OPF* is an optimization problem that finds the setpoints that reduce operational costs while satisfying power flow equations and engineering constraints [3]. To ensure the security of the electric grid, system operators solve *SCOPF problems*, an extension of the OPF with additional constraints that ensure the feasibility of the setpoints pre- and post-contingencies [2]. Since the SCOPF problem was first introduced in [2], several models and algorithms have been proposed in the literature to increase computational efficiency [4].

Many effective algorithms for solving SCOPF problems use reduction methods instead of solving the original problem [5]. These methods exploit the fact that most of the constraints in typical SCOPF problems are not active at the optimal solution, and eliminating the non-active constraints does not change the optimal solution [6]. Iterative methods in [7]–[9] find a subset of the contingencies that dominate the remaining contingencies and solve the problem while only considering the dominated contingencies. Another method to reduce the complexity of SCOPF proposed in [10] identifies umbrella contingencies, defined as the minimum set of contingencies that alter the feasible space once removed. A similar approach proposed in [11] identifies umbrella constraints rather than contingencies. However, the method in [11] requires solving a number of optimization problems equal to the number of constraints, each of the same size as the original SCOPF problem.

Another approach introduced in the literature is to use metaheuristics to solve SCOPF. In [12], the authors propose a scenario reduction method to solve stochastic SCOPF using four metaheuristic algorithms and conclude that particle

[†]Computational Science Center, National Laboratory of the Rockies, Golden, CO, United States. Email: devon.sigler@nlr.gov, bernard.knueven@nlr.gov, Jonathan.Maack@nlr.gov

[‡]Smart Cities Institute, King Abdulaziz City for Science and Technology, Riyadh, Saudi Arabia. Email: malkhraijah@kacst.gov.sa

Authored by the National Laboratory of the Rockies (NLR) for the U.S. Department of Energy (DOE), operated under Contract No. DE-AC36-08GO28308. Support from the Laboratory Directed Research and Development (LDRD) Program at NLR. The views expressed in the article do not necessarily represent the views of the DOE or the U.S. Government.

swarm optimization produces the highest quality solution. Reference [13] proposes a method based on an evolutionary algorithm to partition the contingencies into preventive and corrective control sets. Then, the method iteratively solves SCOPF using Benders decomposition with the preventive control set and solves an optimization problem that minimizes the expected-security-control cost with the corrective control set, while repartitioning the contingencies until the two sets converge. However, metaheuristic methods do not have convergence guaranties and solutions lack transparency, which is necessary for market application.

Rapid advances in the field of machine learning have motivated research into new methods for SCOPF, which can be divided into two categories: (1) finding active constraints and (2) end-to-end solutions. Reference [14] proposes training a neural network that maps the demand to the set of active constraints. Reference [15] proposes an optimization learning framework that uses proxies to map input data to the optimal solution. The results in [15] show a significant increase in the computation speed during the inference stage. However, finding feasible solutions requires a post-processing step and, similarly to metaheuristics, the solutions lack transparency.

Distributed algorithms have been used in the literature to solve SCOPF in parallel. The work in [16] uses the alternating direction method of multipliers to solve SCOPF via decomposing the problem based on contingencies. Reference [17] proposes a distributed method to solve SCOPF based on optimality conditions to decompose the system into subsystems, each with a set of buses and contingencies. Both decomposition methods in [16] and [17] use the B-θ model, which requires including all constraints in the subproblem and prevents the use of efficient reduction methods that are typically employed in central optimization.

In contrast to the methods in [16] and [17], reference [18] proposes a decomposition method to solve SCOPF with a sensitivity-based model using a distributed algorithm. The method in [18] decomposes a system into two subsystems and shows that the decomposition reduces the number of nonzeros in the constraints matrix. However, this method requires additional calculations to allow for multi-area decompositions. Recently, reference [19] proposed a Kron reduction-based decomposition method to solve distributed OPF problems with a sensitivity-based model using a distributed algorithm. The numerical results of the two methods proposed in [18] and [19] show that using sensitivity-based models to solve OPF problems significantly reduces computation time. The method proposed in [18] uses only in two area decomposition, while the method in [19] focuses on distributed OPF problems. This paper builds upon this research direction by using decomposition methods with sensitivity-based models to solve SCOPF with multiple-area decomposition for efficient computation.

B. Contributions

The main contributions of this paper are outlined as follows. (1) Development of a decomposition method to sparsify the constraints matrix of SCOPF problems. The proposed decomposition significantly reduces the number of non-zero entries in the constraints of SCOPF problems by decomposing large systems into smaller subsystems using Kron reduction. Each subsystem model is a projection of the original system model, in which the decomposition maps external variables to local variables via linear operations. To preserve the original problem, the proposed method uses consistency constraints that link the power flows between subsystems. The advantage of the proposed method lies in reducing the number of nonzero entries in the constraint matrix, thus reducing computation time. (2) Demonstration of the effectiveness of the proposed method with a lazy constraints method using large-scale test systems. The lazy constraints method iteratively solves SCOPF problems, considering constraints only when a violation is detected in a previous iteration. The paper considers two large test cases from PGLib-OPF [20], representing the eastern and western interconnections of North America, with up to 78,000 buses and 126,000 lines. The results show that the proposed method solves the SCOPF for the Eastern Interconnection with 78,000 buses and 3,000 contingencies in less than an hour, while the typical B-θ model fails to find a solution even with only 10 contingencies, and the typical PTDF model finds a solution for only up to 500 contingencies in an hour.

C. Organization

The remainder of the paper is organized as follows. Section II presents the background on SCOPF models. Section III describes the proposed sparsification method. Section IV demonstrates the performance of the proposed method compared to common SCOPF models using numerical simulations. Section V presents the conclusions and future work. Detailed numerical results are presented in Appendix A.

II. Background

A. Security-Constraints Optimal Power Flow

SCOPF problems can be preventive or corrective. The preventive SCOPF ensures the feasibility of the post-contingency without changing the setpoints, while the corrective SCOPF allows changes to the post-contingency setpoints using a predefined generation policy. Although the proposed method is applicable for corrective SCOPF, this paper considers preventive SCOPF with contingencies due to line failures.

Consider a power system defined by a graph $G(\mathcal{N}, \mathcal{E})$, where $\mathcal{N}$ and $\mathcal{E}$ are the sets of buses and lines. Define $\mathcal{G}$ and $\mathcal{D}$ as the sets of generators and loads. The set $\mathcal{C} \subset \mathcal{E}$ contains the contingencies indexed from 1 to $|\mathcal{C}|$, and we use the index 0 to denote the pre-contingency. We denote the set of contingencies and the base case as $\mathcal{C}' = \{0\} \cup \mathcal{C}$.

The decision variables are the power injection $p \in \mathbb{R}^{|\mathcal{N}|}$, generator output $g \in \mathbb{R}^{|\mathcal{G}|}$, line flow $f^c \in \mathbb{R}^{|\mathcal{E}|}, c \in \mathcal{C}'$, and phase angle $\theta^c \in \mathbb{R}^{|\mathcal{N}|}, c \in \mathcal{C}'$. The parameters are the line susceptance $b \in \mathbb{R}^{|\mathcal{E}|}$, load demand $d \in \mathbb{R}^{|\mathcal{D}|}$, generator lower and upper bounds $\underline{g}$ and $\overline{g} \in \mathbb{R}^{|\mathcal{G}|}$, and maximum line flow $\bar{f} \in \mathbb{R}^{|\mathcal{E}|}$. We use $h(g) \colon \mathbb{R}^{|\mathcal{G}|} \to \mathbb{R}$ to define the generator cost function, commonly a polynomial or a piece-wise-linear function.

We use $I^G \in \mathbb{R}^{|\mathcal{N}|\times|\mathcal{G}|}$ and $I^D \in \mathbb{R}^{|\mathcal{N}|\times|\mathcal{D}|}$ to denote the generator and load incidence matrices. The value of $I^G_{nk} = 1$ if generator $k \in \mathcal{G}$ is connected to bus $n \in \mathcal{N}$, and $I^G_{nk} = 0$ otherwise. Similarly, the value of $I^D_{nk} = 1$ if load $k \in \mathcal{D}$ is connected to bus $n \in \mathcal{N}$, and $I^D_{nk} = 0$ otherwise. We use $B \in \mathbb{R}^{|\mathcal{N}|\times|\mathcal{N}|}$ to denote the susceptance matrix defined as $B_{ij} = \sum_{(i,k)\in\mathcal{E} \text{ or } (k,i)\in\mathcal{E}} b_{ik}$ if $i = j$, $B_{ij} = -b_{ij}$ if $(i,j) \in \mathcal{E}$ or $(j,i) \in \mathcal{E}$, and $B_{ij} = 0$ otherwise. We also use $B^E \in \mathbb{R}^{|\mathcal{E}|\times|\mathcal{N}|}$ to denote the branch susceptance matrix defined as $B^E_{ei} = b_e$ if $e_1 = i$, $B^E_{ei} = -b_e$ if $e_2 = i$, and $B^E_{ei} = 0$ otherwise. For post-contingency $c \in \mathcal{C}$, we set the line susceptance of line c to $b_c = 0$ and recalculate B^c and B^{Ec} accordingly.

Using this notation, we formulate the preventive SCOPF formulation with the B-θ model as follows.

$$\begin{aligned}
\underset{g,f,\theta,\epsilon}{\text{minimize}} \quad & h(g) + \beta \sum_{c\in\mathcal{C}'} \mathbb{1}^T \epsilon^c, && && \text{(1a)}\\
\text{subject to:} \quad & I^G g - I^D d = B^c \theta^c, && \forall c \in \mathcal{C}', && \text{(1b)}\\
& f^c = B^{Ec}\theta^c, && \forall c \in \mathcal{C}', && \text{(1c)}\\
& \underline{g} \leq g \leq \overline{g}, && && \text{(1d)}\\
& -\overline{f} - \epsilon^c \leq f^c \leq \overline{f} + \epsilon^c, && \forall c \in \mathcal{C}', && \text{(1e)}\\
& \theta_0 = 0, && && \text{(1f)}
\end{aligned}$$

where $\mathbb{1}$ is a vector of ones with the appropriate size. We introduce slack variables $\epsilon^c \in \mathbb{R}^{|\mathcal{E}|}, c \in \mathcal{C}'$ for line violations with a high penalty parameter $\beta > 0$. The objective function (1a) minimizes the generation cost and the line violations. Equalities (1b) and (1c) are the DC approximation of the power flow equations, inequalities (1d) and (1e) bound the generator outputs and line flows, and (1f) sets the reference angle.

The size of the SCOPF problem in (1) rapidly increases when considering more contingencies. Considering a new contingency is equivalent to adding a new OPF instance with the contingency parameters to the SCOPF problem.

A more tractable equivalent problem uses sensitivity matrices, namely the power transfer distribution factors (PTDF) and line outage distribution factors (LODF) [21]. The *PTDF model* uses the sensitivities of the line flows with respect to the power injections to express the power flow equations without phase angle variables. Moreover, instead of calculating the line flow at each contingency, the LODF uses the PTDF calculation to find the post-contingency line flow as a function of the pre-contingency line flow. We denote the PTDF matrix as $H \in \mathbb{R}^{|\mathcal{E}|\times|\mathcal{N}|}$, defined as

$$H = B^E B^{-1}, \tag{2}$$

and the LODF matrix $L \in \mathbb{R}^{|\mathcal{E}|\times|\mathcal{C}|}$, defined for all $e \in \mathcal{E}$ and $c \in \mathcal{C}$ as

$$L_{ec} = \begin{cases} \dfrac{H_{ec_1} - H_{ec_2}}{1 - (H_{cc_1} - H_{cc_2})}, & e \neq c, \\ -1, & e = c. \end{cases} \tag{3}$$

where $c = (c_1, c_2) \in \mathcal{E}$ is the contingency line that connects bus c_1 and c_2. Note that the susceptance matrix is singular. Thus, we invert a reduced version that omits an arbitrary reference bus. The reference bus acts as a slack for any mismatch in power injections.

Using the PTDF and LODF matrices, we formulate the preventive SCOPF with the PTDF model as follows.

$$\begin{aligned}
\underset{g,f,\epsilon}{\text{minimize}} \quad & h(g) + \beta \sum_{c\in\mathcal{C}'} \mathbb{1}^T \epsilon^c, && && \text{(4a)}\\
\text{subject to:} \quad & p = I^G g - I^D d && && \text{(4b)}\\
& \mathbb{1}^T p = 0, && && \text{(4c)}\\
& f^0 = Hp, && && \text{(4d)}\\
& f^c = f^0 + L_{:c} f^0_c, && \forall c \in \mathcal{C} && \text{(4e)}\\
& \underline{g} \leq g \leq \overline{g}, && && \text{(4f)}\\
& -\overline{f} - \epsilon^c \leq f^c \leq \overline{f} + \epsilon^c, && \forall c \in \mathcal{C}'. && \text{(4g)}
\end{aligned}$$

Unlike the B-θ, where adding a contingency adds a new OPF instance, the PTDF model only adds constraints (4e) and (4g). Moreover, since few line flow limits will be active at the optimal solution, several efficient methods focus on finding the active sets. The challenge with the PTDF model arises from the density of the PTDF matrix H, leading to a dense constraints matrix due to equality (4d). The next section describes a method based on Kron reduction to impose sparsity on the PTDF matrix, leading to faster computation.

III. Sparsification Method

This section presents a sparsification method for the PTDF model. We first present a decomposition method based on Kron reduction to decompose the system into multiple subsystems, each representing a reduced version of the original system. Next, we propose additional constraints to connect the reduced systems and ensure consistency with the original problem. Finally, we present the decomposed PTDF model of the SCOPF.

A. Reduced Subsystems

The first step of the proposed sparsification method is to decompose the system into multiple equivalent subsystems using Kron reduction, a well-known technique in electric circuit and power systems analysis [22], [23]. Each subsystem represents a projected version of the original system into the local variables of the subsystem.

Considering a power system represented by the graph $G(\mathcal{N}, \mathcal{E})$. We partition the buses into mutually exclusive and exhaustive subsets over the set of areas $\mathcal{A}$. Preferably, the partitioning should be based on the proximity of the buses in the graph and produce relatively equal sizes for each subset. The partitioning could represent a physical or regional distribution of the buses, e.g., operational regions. We then use Kron reduction to find a reduced representation of the original system that only includes the buses inside and on the boundary of each area as follows. The boundary buses are outside the area and connected to a bus within the area.

For each area $a \in \mathcal{A}$, we divide the buses of the original system into three subsets $\mathcal{N}^a_i$, $\mathcal{N}^a_b$, and $\mathcal{N}^a_e$, the subsets of internal, boundary, and external buses, with corresponding power injections p^i, p^b, and p^e, respectively. The set of internal buses is defined by the partitioning, and the set of boundary buses includes any bus that is connected to an internal bus by a line, while the remaining busses are contained in the set of external buses. Using these definitions, we rewrite the power balance equations as follows.

$$\begin{bmatrix} p^i \\ p^b \\ p^e \end{bmatrix} = \begin{bmatrix} B^{ii} & B^{ib} & 0 \\ B^{bi} & B^{bb} & B^{be} \\ 0 & B^{eb} & B^{ee} \end{bmatrix} \begin{bmatrix} \theta^i \\ \theta^b \\ \theta^e \end{bmatrix}.$$

We then use a Gaussian elimination step on the rows corresponding to the external buses in $\mathcal{N}_e^a$ and write the power balance equation of the reduced system as follows.

$$p^a = \begin{bmatrix} p^i \\ p^b + A^a p^e \end{bmatrix} = \begin{bmatrix} B^{ii} & B^{ib} \\ B^{bi} & B^{bb} + A^a B^{eb} \end{bmatrix} \begin{bmatrix} \theta^i \\ \theta^b \end{bmatrix} = B^a \theta^a, \quad (5)$$

where $A^a = -B^{be}\,(B^{ee})^{-1}$ is the accompanying matrix. The power balance equation (5) only depends on the phase angles of the reduced buses θ^i and θ^b. Note that the power injection vector p^a represents an equivalent power injection rather than an actual power injection.

Applying the Kron reduction to all areas $a \in \mathcal{A}$, we rewrite the power balance equations as follows.

$$\begin{bmatrix} p^1 \\ p^2 \\ \vdots \\ p^{|\mathcal{A}|} \end{bmatrix} = \begin{bmatrix} B^1 & 0 & \dots & 0 \\ 0 & B^2 & \dots & 0 \\ \vdots & \vdots & \ddots & \vdots \\ 0 & 0 & \dots & B^{|\mathcal{A}|} \end{bmatrix} \begin{bmatrix} \theta^1 \\ \theta^2 \\ \vdots \\ \theta^{|\mathcal{A}|} \end{bmatrix}. \quad (6)$$

The power balance equation (6) represents separable areas. However, the power injection vector p^a and the phase angles vector θ^a of each area contain variables that appear in other areas. To ensure consistency in those shared variables, we impose additional constraints, described next.

B. Consistency Constraints

Considering the reduced subsystem $a \in \mathcal{A}$. Recall $\mathcal{N}_i^a, \mathcal{N}_b^a$, and $\mathcal{N}_e^a \subset \mathcal{N}$ are the subsets of internal, boundary, and external buses from (5) with corresponding actual power injection vectors p^i, p^b, and p^e prior to Kron reduction. Using the power balance of the reduced system (5), the power injection of any bus $n \in \mathcal{N}_b^a$ in the boundary is

$$p_n^a = p_n + \sum_{v \in \mathcal{N}_e^a} A_{nv}^a \, p_v. \quad (7)$$

Since $\mathcal{N}_b^a$ is the area a boundary buses, there is another area $a' \in \mathcal{A}$ for each bus $n \in \mathcal{N}_b^a$ such that $n \in \mathcal{N}_i^{a'}$ and $p_n^{a'} = p_n$. Similarly, for any bus $v \in \mathcal{N}_e^a$, there is a unique area $k \in \mathcal{A}$ such that $v \in \mathcal{N}_i^k$ and $p_v = p_v^k$. Substituting the values of p_n and p_v into (7), we get

$$p_n^a = p_n + \sum_{k \in \mathcal{A}\setminus\{a\}} \sum_{v \in \mathcal{N}_e^a \cap \mathcal{N}_i^k} A_{nv}^a \, p_v, \quad (8a)$$

$$p_n^a = p_n^{a'} + \sum_{k \in \mathcal{A}\setminus\{a\}} \sum_{v \in \mathcal{N}_e^a \cap \mathcal{N}_i^k} A_{nv}^a \, p_v^k. \quad (8b)$$

The first equality (8a) distributes $\mathcal{N}_e^a$ to the internal buses of the other areas defined by the sets $\mathcal{N}_i^k$ for $k \in \mathcal{A} \setminus \{a, a'\}$. The second equality (8b) uses (5) to substitute for the actual value of the power injection p_n by $p_n^{a'}$ and p_v by p_v^k.

Using the consistency constraints (8b) for all buses $n \in \mathcal{N}_b^a, a \in \mathcal{A}$ ensures that the power balance equation (6) is equivalent to the actual system power balance equation. For more details on the equivalence, we refer the reader to our previous work in [19, Theorem 1].

C. Decomposed Security-Constraints Optimal Power Flow

To formulate the preventive SCOPF using the proposed decomposition in the previous section, we first introduce auxiliary variables representing the power flow between areas. Let $s^a \in \mathbb{R}^{|\mathcal{N}_b^a|}$ be auxiliary variables representing the power flow from/to area a, and $I^{Sa} \in \mathbb{R}^{|\mathcal{N}^a| \times |\mathcal{N}_b^a|}$ is the corresponding incidence matrix. We then calculate the local PTDF matrices for each area using (2) with the local susceptance matrix B^a and the local line susceptance matrix B^{Ea} that includes only internal lines. Since the PTDF matrix implicitly uses a reference bus to compensate for mismatches in power injections, we select a common reference bus for all areas, i.e., the reference bus is shared by all areas. Thus, the PTDF matrix of $a \in \mathcal{A}$ is $H^a = (B^a)^{-1} B^{Ea}$. For the local LODF matrix $L^a, a \in \mathcal{A}$, we use the system-wide LODF and take the rows corresponding to the internal lines for each area. Note that the local LODF matrix L^a relates the post-contingency line flow of the internal lines to the pre-contingency flow of the contingency line, which might not be an internal line. We use $a_c \in \mathcal{A}, c \in \mathcal{C}$ to denote the area of the contingency line. Using the proposed decomposition, we formulate the preventive SCOPF as follows.

$$\begin{aligned}
&\underset{g,s,f,\epsilon}{\text{minimize}} && \sum_{a \in \mathcal{A}} \left(h^a(g^a) + \beta \sum_{c \in \mathcal{C}'} \mathbb{1}^T \epsilon^{ca} \right), && (9a)\\
&\text{subject to:} && \forall a \in \mathcal{A}: && \\
& && p^a = I^{Ga} g^a - I^{Da} d^a + I^{Sa} s^a, && (9b)\\
& && \mathbb{1}^T p^a = 0, && (9c)\\
& && f^{0a} = H^a p^a, && (9d)\\
& && f^{ca} = f^{0a} + L^a_{:c} f_c^{0a_c}, \qquad \forall c \in \mathcal{C}, && (9e)\\
& && \underline{g}^a \le g^a \le \overline{g}^a, && (9f)\\
& && -\overline{f}^a - \epsilon^{ca} \le f^{ca} \le \overline{f}^a + \epsilon^{ca}, \qquad \forall c \in \mathcal{C}', && (9g)\\
& && \text{and (8b)}, \qquad \forall n \in \mathcal{N}_b^a. &&
\end{aligned}$$

The constraints in (9) are separable based on areas, except for the post-contingency line flow expression (9e) and the consistency constraints (8b) that couple variables from different areas. Moreover, the post-contingency line flow expression (9e) is sparse since it only couples two variables, while the consistency constraints (8b) are dense. However, the density of (8b) is much lower than that of the original power balance equation (4d). We use a lazy constraints method to solve the decomposed SCOPF, where we iteratively solve (9) without the line flow constraints (9d), (9e), and (9g), and add the corresponding constraints when a violation is detected. The overall flow of the decomposed SCOPF with the lazy constraints method is shown in Algorithm 1. We use $\mathcal{T} \subset \mathcal{E} \times \mathcal{C}'$ to denote the set of line flow constraints that are considered when solving (9), i.e., if $(e, c) \in \mathcal{T}$, we add the corresponding constraints (9d), (9e), and (9g) to the problem.

TABLE I
NUMBER OF COMPONENT, TOTAL AVAILABLE GENERATION, AND TOTAL DEMAND OF THE TEST CASES FROM PGLIB-OPF

Case	Bus	Line	Gen.	Gen. Cap. (p.u.)	Demand (p.u.)
20758_epigrids	20758	33343	2174	2023.04	1208.86
78484_epigrids	78478	126015	6773	8249.16	5149.57

IV. NUMERICAL RESULTS

This section presents numerical simulations for solving SCOPF, comparing the B-θ, typical PTDF, and proposed models performance. We ran a simulation using two large-scale synthetic test systems from PGLib-OPF [20] that represent the North American western and eastern interconnections: `case20758_epigrids` and `case78484_epigrids`. The number of components, generation capacity, and total demand of the two test systems are shown in Table IV. We ran the simulation on Kestrel, a high performance computing platform at the National Laboratory of the Rockies, with a single Intel Xeon CPU with 104 cores and 256GB of memory. The simulation was run in the Julia programming language and used JuMP v1.10.5 to build the models and Gurobi v12.0.3 to solve the models.

The core feature of the proposed decomposition is to increase the sparsity of the SCOPF with the PTDF models. To show the change in the sparsity of the constraints matrix, we focus on the equality constraints because the other constraints are sparse. Moreover, we only show the base case line flows, since the post-contingency line flow constraints are the same for the typical and proposed models. Fig. 1 shows the non-zeros of the equality constraints for `case20758_epigrids` with the typical PTDF on the left and the decomposed PTDF on the right. The typical PTDF constraints matrix consists of a dense block containing the PTDF entries and a diagonal block that links the line flow with the power injections. The constraints matrix of the decomposed PTDF consists of blocks representing the partition of the original system and a dense block at the top corresponding to the consistency constraints. Each block has the same structure as the full typical PTDF equality but is of a much smaller size. Assuming the number

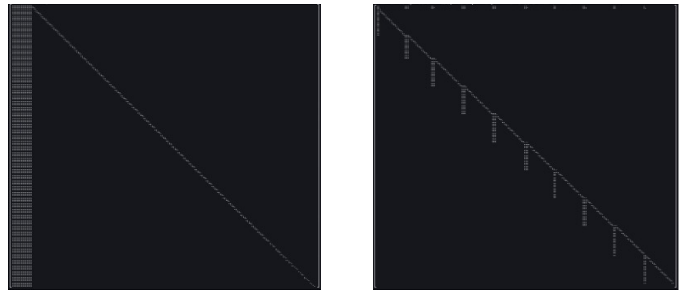

Fig. 1. The sparsity pattern of the equality constraints of typical PTDF model (4) in the left and decomposed PTDF model (9) in the right for `case20758_epigrids`. The left figure shows the non-zeros of equalities (4c) and (4d) with 33,344 rows, 35,517 columns, and 65,933,978 non-zeros. The right figure shows the non-zeros of equalities (9c), (9d) and (8b) after substituting for the power injection using (9b) with 34,005 rows, 36,168 columns, and 8,743,139 non-zeros.

of areas is $|\mathcal{A}|$ and each area has an equal number of generators and lines, the proposed method reduces the number of non-zeros in the dense block of the typical PTDF matrix by a percentage of $100 * \left(\frac{|\mathcal{A}|-1}{|\mathcal{A}|}\right)$. However, the trade-off is that the proposed method adds a dense block corresponding to the consistency constraints. Nonetheless, the reduction in the number of non-zeros in the decomposed model is significant, negating the increase in the number of variables and constraints.

In Fig. 1, the number of non-zeros for the typical PTDF equality constraints (4c) and (4d) is 65,933,978, while the proposed decomposition equalities (9c), (9d), and (8b) have 8,743,139 non-zeros. Thus, the equality constraints in the proposed decomposition (9) have 87% fewer non-zeros compared to the PTDF model (4). Note that the total number of columns and rows in the proposed decomposition is higher than that of the typical PTDF model due to the addition of the auxiliary variables $s^a, a \in \mathcal{A}$ and the consistency constraints (8b).

We solved the SCOPF for the test cases while varying the number of contingencies from 10 to 10,000. We selected the contingencies based on the power flow in the base case and only considered contingencies that do not cause islanding. We use the lazy constraints method to solve the typical PTDF (4) and decomposed PTDF (9) models as depicted in Algorithm 1. The computation time and the actual solver time for `case20758_epigrids` are shown in Fig. 2 and 3, respectively. The solver time is the wall-clock time spent on calling the solver and solving the problem, while the total time includes the time spent on building the model, evaluating the line flow, adding violated constraints, and the solver time.

Comparing the performance of the three models, the B-θ solves SCOPF with up to 300 contingencies within 1-hour, while the typical PTDF solves SCOPF for 10,000 contingencies in 1507 seconds, and the decomposed PTDF does so in 620 seconds. Both the total computation time and solver time of the B-θ model rapidly increase as we add more contingencies because adding a contingency is equivalent to adding a new OPF instance. On the other hand, the results show a slower increase in computation time as we increase the number of contingencies for the two PTDF models, which demonstrates the effectiveness of the lazy constraints method.

Algorithm 1 Decomposed SCOPF with Lazy Constraints

Initialize $t = 1, \mathcal{T}^0 = \emptyset$
Compute A^a and $B^a, \forall a \in \mathcal{A}$ using (5)
Compute $H^a, \forall a \in \mathcal{A}$ and $L_{ec}, \forall e \in \mathcal{E}, c \in \mathcal{C}$ using (2) and (3)
repeat
  Solve (9) using T^{t-1} line flow constraints
  Compute $f_e^c, \forall e \in \mathcal{E}, c \in \mathcal{C}'$ using (9d) and (9e)
  Set $\mathcal{F} = \{(e, c) \in \mathcal{E} \times \mathcal{C}' \colon -\overline{f}_e \geq f_e^c \text{ or } f_e^c \geq \overline{f}_e\}$
  if $\mathcal{F} = \emptyset$ **then**
    solution is optimal **Terminate**
  end if
  Set $\mathcal{T}^t = \mathcal{T}^{t-1} \cup \mathcal{F}$
  $t \leftarrow t + 1$
until

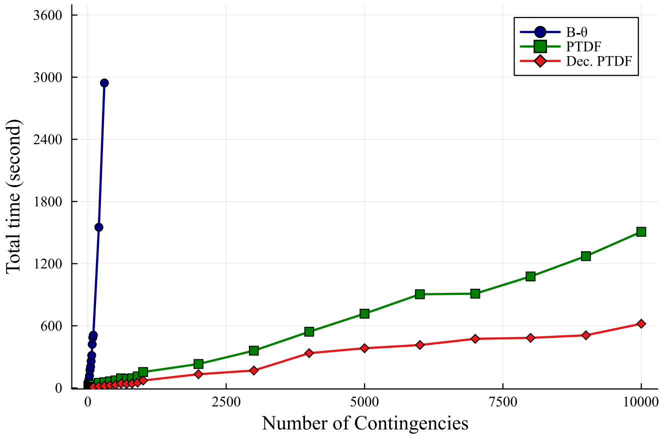

Fig. 2. Total computation time of the SCOPF with 10 to 10,000 contingencies with the B-θ, typical PTDF, and decomposed PTDF models for `case20758_epigrids`.

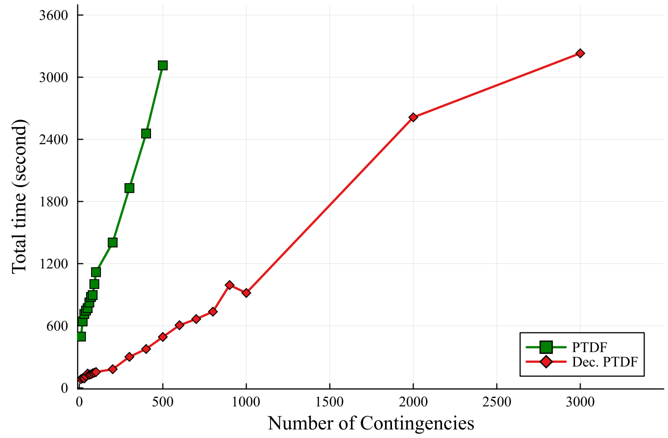

Fig. 4. Total computation time of the SCOPF with 10 to 3,000 contingencies with the typical and decomposed PTDF models for `case78484_epigrids`.

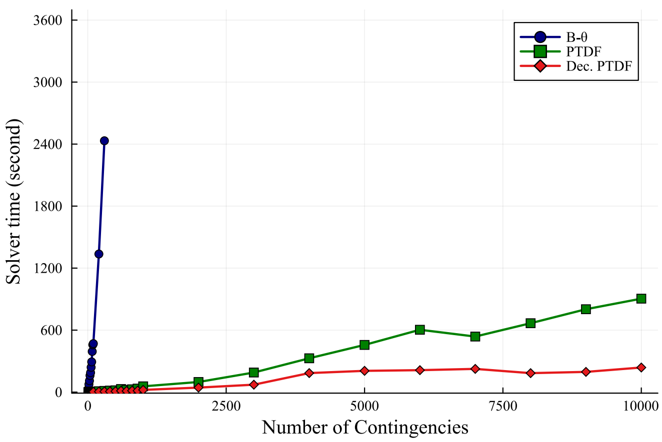

Fig. 3. Solver time of the SCOPF with 10 to 10,000 contingencies with the B-θ, typical PTDF, and decomposed PTDF models for `case20758_epigrids`.

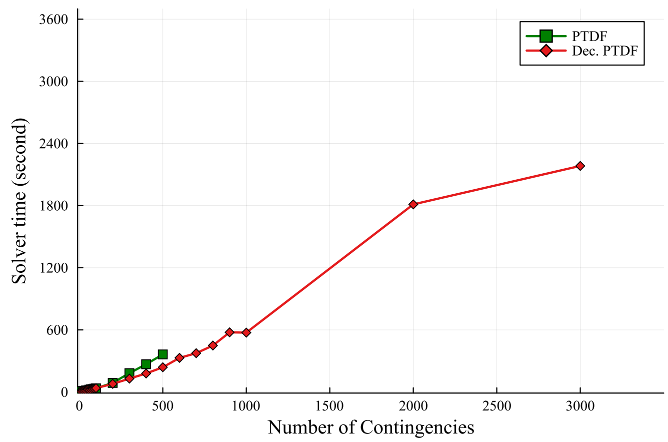

Fig. 5. Solver time of the SCOPF with 10 to 3,000 contingencies with the typical and decomposed PTDF models for `case78484_epigrids`.

The total computation time and the solver time of the SCOPF with the typical and decomposed PTDF models, while varying the number of contingencies for `case78484_epigrids`, are shown in Fig. 4 and 5. The SCOPF with the B-θ model failed to find a solution within 1 hour, even with only 10 contingencies. Comparing the two PTDF models, the decomposed PTDF solves up to 3,000 contingencies in 3,200 seconds, while the typical PTDF model only finds a solution for problems with up to 500 contingencies within 1 hour. The detailed results of the two test cases are shown in Table II and Table III in the Appendix.

The significant increase in the total computation time is due to the time needed to evaluate the constraints and add the violated constraints to the model. We note here that there are more efficient methods to evaluate the constraints. However, even if we reduce the constraints evaluation time, the solver time of the proposed decomposition is still lower than that of the typical PTDF model. Moreover, the difference in the constraints matrix structures impacts the computation time since we evaluate the constraints using much smaller matrices in the decomposed PTDF model compared to the typical PTDF model. Specifically, assuming a decomposition of $\mathcal{A}$ areas with an equal number of generators and lines, the decomposed PTDF evaluates $|\mathcal{A}|$ matrices, each with $\frac{|\mathcal{E}|\times|\mathcal{G}|}{|\mathcal{A}|^2}$ entries, compared to a single matrix with $|\mathcal{E}| \times |\mathcal{G}|$ entries. Although the number of constraint evaluations is almost the same, the number of multiplications in each constraint evaluation in the decomposed model is $\frac{1}{|\mathcal{A}|}$ of the typical PTDF model, causing a significant reduction in computation time for large systems.

V. Conclusion

This paper presents a decomposition method to sparsify SCOPF with a sensitivity-based model. The core feature of the proposed method is reducing the number of non-zeros in the constraints matrix. Using the proposed method to decompose a system into 10 areas of balanced size reduces the number of non-zeros by 90% compared to typical SCOPF models. However, the trade-off is that the proposed method adds auxiliary variables and consistency constraints to ensure the retention of the original system. Nonetheless, the number of non-zeros with the additional variables and constraints is 86%

less than that of the typical SCOPF models. Sparsifying the constraints matrix significantly reduces the computation time. The numerical results on two of the largest test cases in the PGLib-OPF, representing the Western and Eastern interconnections of North America, show that the computational time of the proposed method is 7 times less than the typical SCOPF models.

Network constraints appear in many applications throughout optimization problems in power systems. A future research direction is to apply the proposed method to large-scale problems, such as multi-period OPF and stochastic OPF, in addition to problems with binary variables, such as unit commitment. Although the proposed method requires linear power flow models, non-linear ACOPF problems have been solved efficiently using successive linearization methods, which positions it as potential future work for the proposed method. Lastly, the proposed decomposition can be directly used to solve SCOPF in distributed settings with a parallel implementation.

APPENDIX

The detailed computation times for the B-θ, PTDF, and decomposed PTDF models for `case20758_epigrids` and `case78484_epigrids` test systems, from PGLib-OPF [20], are shown in Table II and Table III, respectively. The first column shows the number of contingencies, and the second column shows the objective function value of the optimal solution. For each model, the data columns show the data reprocessing time, the solve columns show the time spent solving the problem by the solver, and the total column shows the time spent on building the model, evaluating constraint violations, adding violated constraints to the model, and the solve time. All the computation times are wall-clock time measured in seconds. We use "T.L." to indicate that the algorithm failed to find a solution within the time limit, which is 1 hour in this simulation.

REFERENCES

[1] U.S.-Canada Power System Outage Task Force, "Final report on the August 14, 2003 blackout in the United States and Canada: Causes and recommendations," tech. rep., 2008.

[2] O. Alsac and B. Stott, "Optimal load flow with steady-state security," *IEEE Transactions on Power Apparatus and Systems*, vol. PAS-93, no. 3, pp. 745–751, 1974.

[3] H. W. Dommel and W. F. Tinney, "Optimal power flow solutions," *IEEE Transactions on power apparatus and systems*, no. 10, pp. 1866–1876, 2007.

[4] S. Li, J. Lu, Z. Yu, Y. Dai, S. Liu, W. Tang, and Y. Guo, "A review of security-constrained optimal power flow calculation method," in *The Third International Conference on Artificial Intelligence, Information Processing and Cloud Computing (AIIPCC)*, 2022.

[5] F. Capitanescu, J. M. Ramos, P. Panciatici, D. Kirschen, A. M. Marcolini, L. Platbrood, and L. Wehenkel, "State-of-the-art, challenges, and future trends in security constrained optimal power flow," *Electric power systems research*, vol. 81, no. 8, pp. 1731–1741, 2011.

[6] D. G. Luenberger and Y. Ye, *Linear and nonlinear programming*, vol. 2. Springer, 1984.

[7] F. Capitanescu, M. Glavic, D. Ernst, and L. Wehenkel, "Contingency filtering techniques for preventive security-constrained optimal power flow," *IEEE Transactions on Power Systems*, vol. 22, no. 4, pp. 1690–1697, 2007.

[8] F. Capitanescu and L. Wehenkel, "A new iterative approach to the corrective security-constrained optimal power flow problem," *IEEE Transactions on Power Systems*, vol. 23, no. 4, pp. 1533–1541, 2008.

[9] S. Lv, S. Chen, Z. Wei, and G. Sun, "Security-constrained optimal traffic-power flow with adaptive convex relaxation and contingency filtering," *IEEE Transactions on Transportation Electrification*, vol. 9, no. 1, pp. 1605–1617, 2023.

[10] F. Bouffard, F. D. Galiana, and J. M. Arroyo, "Umbrella contingencies in security-constrained optimal power flow," in *15th Power systems computation conference (PSCC)*, vol. 5, pp. 0885–8950, 2005.

[11] A. J. Ardakani and F. Bouffard, "Identification of umbrella constraints in DC-based security-constrained optimal power flow," *IEEE Transactions on Power Systems*, vol. 28, no. 4, pp. 3924–3934, 2013.

[12] S. Das, B. B. Das, and A. Sengupta, "Security-constrained stochastic optimal power flow analysis using optimally reduced scenarios for wind generation," *Electrical Engineering*, vol. 107, pp. 7685–7707, 2025.

[13] Y. Xu, H. Yang, R. Zhang, Z. Y. Dong, M. Lai, and K. P. Wong, "A contingency partitioning approach for preventive-corrective security-constrained optimal power flow computation," *Electric Power Systems Research*, vol. 132, pp. 132–140, 2016.

[14] S. Liu, Y. Guo, W. Tang, H. Sun, and W. Huang, "Predicting active constraints set in security-constrained optimal power flow via deep neural network," in *2021 IEEE Power & Energy Society General Meeting (PESGM)*, 2021.

[15] F. Jiang, X. Li, and P. Van Hentenryck, "A deep neural network-based frequency predictor for frequency-constrained optimal power flow," in *2025 IEEE Industry Applications Society Annual Meeting (IAS)*, 2025.

[16] L. Liu, A. Khodaei, W. Yin, and Z. Han, "A distribute parallel approach for big data scale optimal power flow with security constraints," in *IEEE International Conference on Smart Grid Communications (SmartGridComm)*, pp. 774–778, 2013.

[17] J. Mohammadi, G. Hug, and S. Kar, "Agent-based distributed security constrained optimal power flow," *IEEE Transactions on Smart Grid*, vol. 9, no. 2, pp. 1118–1130, 2016.

[18] A. S. Xavier, S. S. Dey, and F. Qiu, "Decomposable formulation of transmission constraints for decentralized power systems optimization," *INFORMS Journal on Computing*, vol. 36, no. 6, pp. 1562–1578, 2024.

[19] M. Alkhraijah, D. Sigler, and D. K. Molzahn, "A decomposition method for solving sensitivity-based distributed optimal power flow," *Electric Power Systems Research*, vol. 263, p. 113608, 2027. Presented at *24nd Power System Computation Conference (PSCC 2026)*.

[20] IEEE PES Task Force on Benchmarks for Validation of Emerging Power System Algorithms, "The Power Grid Library for benchmarking AC optimal power flow algorithms," arXiv:1908.02788, 2019.

[21] J. Guo, Y. Fu, Z. Li, and M. Shahidehpour, "Direct calculation of line outage distribution factors," *IEEE Transactions on Power Systems*, vol. 24, no. 3, pp. 1633–1634, 2009.

[22] G. Kron, *Diakoptics: Piecewise solutions of large scale system*. London: Macdonald, 1963.

[23] F. Dorfler and F. Bullo, "Kron reduction of graphs with applications to electrical networks," *IEEE Transactions on Circuits and Systems I: Regular Papers*, vol. 60, no. 1, pp. 150–163, 2012.

TABLE II
COMPUTATION TIME FOR SOLVING SCOPF WITH CASE20758_EPIGRIDS AND VARIOUS NUMBER OF CONTINGENCIES

Contingencies	Optimal Objective ($)	B–θ			PTDF			Dec. PTDF		
		Data (s)	Solve (s)	Total (s)	Data (s)	Solve (s)	Total (s)	Data (s)	Solve (s)	Total (s)
10	2.57×10^6	0.34	31.38	34.84	11.00	0.33	23.76	27.84	1.42	6.23
20	2.58×10^6	0.30	75.48	81.33	10.38	0.58	24.73	28.87	1.24	6.13
30	2.58×10^6	0.29	110.38	117.38	10.43	1.38	27.18	28.70	1.51	6.71
40	2.58×10^6	0.32	160.67	172.09	10.55	2.32	28.85	29.15	1.83	7.06
50	2.58×10^6	0.45	188.63	204.75	11.33	2.79	29.01	28.75	2.20	8.19
60	2.58×10^6	0.43	240.13	257.84	11.20	2.86	30.36	28.74	2.19	8.22
70	2.58×10^6	0.40	292.62	313.67	11.11	2.99	30.03	28.44	2.14	8.60
80	2.58×10^6	0.45	393.42	421.14	11.29	3.15	30.71	29.18	2.30	9.14
90	2.58×10^6	2.98	458.04	485.84	11.21	3.26	31.81	29.21	2.64	9.24
100	2.58×10^6	0.43	469.39	509.45	11.33	3.51	32.18	28.85	2.45	9.31
200	2.59×10^6	0.40	1336.46	1551.33	11.46	8.89	49.05	28.87	4.59	15.03
300	2.70×10^6	0.92	2432.32	2944.36	11.77	12.08	55.31	29.25	5.87	19.30
400	2.72×10^6	1.53	2977.29	4034.27	11.45	14.95	63.10	31.84	6.48	24.93
500	2.72×10^6	T.L.	T.L.	T.L.	11.85	17.68	72.62	31.84	8.10	29.00
600	2.73×10^6	T.L.	T.L.	T.L.	11.80	30.02	92.40	32.02	12.68	41.86
700	2.73×10^6	T.L.	T.L.	T.L.	11.75	22.55	86.88	32.92	11.01	38.43
800	2.76×10^6	T.L.	T.L.	T.L.	11.59	27.39	93.22	32.79	13.93	42.09
900	2.76×10^6	T.L.	T.L.	T.L.	11.92	34.34	111.01	31.92	13.86	51.73
1000	2.77×10^6	T.L.	T.L.	T.L.	11.61	56.06	153.49	32.05	21.57	71.65
2000	2.88×10^6	T.L.	T.L.	T.L.	11.40	98.01	230.98	31.45	43.88	132.35
3000	2.89×10^6	T.L.	T.L.	T.L.	12.07	189.76	359.76	32.24	72.01	168.21
4000	2.90×10^6	T.L.	T.L.	T.L.	11.71	327.46	542.57	33.38	184.32	335.83
5000	2.90×10^6	T.L.	T.L.	T.L.	11.80	456.76	716.76	32.96	205.98	383.26
6000	2.90×10^6	T.L.	T.L.	T.L.	11.99	603.53	904.33	33.14	212.60	414.28
7000	2.90×10^6	T.L.	T.L.	T.L.	12.14	537.73	910.06	33.52	224.87	474.26
8000	2.91×10^6	T.L.	T.L.	T.L.	12.31	666.85	1076.27	32.51	183.75	483.64
9000	2.91×10^6	T.L.	T.L.	T.L.	12.51	802.22	1272.50	34.88	195.83	508.26
10000	2.91×10^6	T.L.	T.L.	T.L.	12.73	904.51	1507.39	35.21	238.20	619.62

TABLE III
COMPUTATION TIME FOR SOLVING SCOPF WITH CASE78484_EPIGRIDS AND VARIOUS NUMBER OF CONTINGENCIES

Contingencies	Optimal Objective ($)	B–θ			PTDF			Dec. PTDF		
		Data (s)	Solve (s)	Total (s)	Data (s)	Solve (s)	Total (s)	Data (s)	Solve (s)	Total (s)
10	1.52×10^7	T.L.	T.L.	T.L.	173.14	7.56	495.66	313.25	9.70	85.08
20	1.52×10^7	T.L.	T.L.	T.L.	163.03	10.25	642.15	316.27	13.22	93.12
30	1.52×10^7	T.L.	T.L.	T.L.	173.38	12.48	713.48	317.79	15.31	92.20
40	1.52×10^7	T.L.	T.L.	T.L.	177.51	15.48	746.58	327.99	18.26	112.45
50	1.52×10^7	T.L.	T.L.	T.L.	171.15	16.76	770.02	381.27	23.28	138.70
60	1.52×10^7	T.L.	T.L.	T.L.	175.09	23.31	824.59	346.63	23.52	127.07
70	1.53×10^7	T.L.	T.L.	T.L.	185.56	26.82	877.87	355.81	26.74	131.87
80	1.53×10^7	T.L.	T.L.	T.L.	185.91	28.76	896.44	354.64	31.01	141.47
90	1.53×10^7	T.L.	T.L.	T.L.	181.63	33.19	1002.98	354.55	33.74	147.17
100	1.53×10^7	T.L.	T.L.	T.L.	176.17	35.85	1117.95	330.84	37.80	153.41
200	1.55×10^7	T.L.	T.L.	T.L.	175.89	88.26	1403.95	314.78	79.03	180.93
300	1.56×10^7	T.L.	T.L.	T.L.	176.27	182.26	1929.48	336.60	129.66	300.00
400	1.57×10^7	T.L.	T.L.	T.L.	183.68	268.43	2456.46	538.56	179.19	375.78
500	1.58×10^7	T.L.	T.L.	T.L.	179.89	363.20	3114.28	362.57	239.33	491.93
600	1.61×10^7	T.L.	T.L.	T.L.	T.L.	T.L.	T.L.	412.02	329.81	605.57
700	1.67×10^7	T.L.	T.L.	T.L.	T.L.	T.L.	T.L.	420.93	375.05	664.84
800	1.71×10^7	T.L.	T.L.	T.L.	T.L.	T.L.	T.L.	319.14	449.17	736.29
900	1.72×10^7	T.L.	T.L.	T.L.	T.L.	T.L.	T.L.	337.33	576.43	993.40
1000	1.74×10^7	T.L.	T.L.	T.L.	T.L.	T.L.	T.L.	308.58	573.67	916.84
2000	1.90×10^7	T.L.	T.L.	T.L.	T.L.	T.L.	T.L.	305.40	1812.00	2612.62
3000	1.99×10^7	T.L.	T.L.	T.L.	T.L.	T.L.	T.L.	320.46	2183.21	3230.85
4000	T.L.	T.L.	T.L.	T.L.	T.L.	T.L.	T.L.	T.L.	T.L.	T.L.

I. REVIEW #158A

A. Paper summary

The paper proposes an approach that increases the sparsity of the PTDF matrix for applications in SCOPF. The method is implemented and demonstrated on real-world systems showing improved computation speed compared to the original problem formulation with the full PTDF matrix.

B. Comments for authors

The paper is well written, i.e. the reader can easily follow the derivations and the proposed steps in the method.

- The method is implemented and tested on real-world systems and it shows clearly improved performance compared to the "typical" PTDF method.
- The description of the type of buses could be improved, particularly the boundary buses. There is ambiguity with respect to if the boundary buses are within the area but connect to buses outside or if they are outside the area and connect to buses within the area. The statement "... is connected to an internal bus by a line ..." is also ambiguous as it implies that it is not possible to connect to two nodes within the area. => a figure would help clarify the definitions
- Fig 1. is hard to read and interpret as it seems that black is used to indicate that it is a zero value and gray for non-zero value => please improve the legibility of the figure;
- It is not intuitively clear why the matrices look the way they do in Fig. 1. Some of the explanation is hidden in the caption, but even with that it is not entirely clear. It would probably be helpful if you give an improved explanation, including references to constraints also in the text.
- The proposed approach is compared to the brute force approach of including all the constraints and the full PTDF in the problem formulation or using the $\mathbf{B} - \theta$ formulation. It is of course not reasonable to ask for a comparison to all existing approaches but it would be good to provide a comparison to another commonly used approach, e.g. using Benders decomposition.
- on page 4: the word sustenance matrix is used but this probably should be susceptance matrix
- there seem to be a few wrong references:
  - page 4 at the bottom: this probably shouldn't be (9c)
  - page 5: there are two references to Fig. IV which does not exist => should be Fig. 1
  - page 5: "... as depicted in 1." => something is missing here
- Typo on page 4: "... and the phase angles vector θ^a or ..."; the "or" probably should be a "of"

C. Summarize your recommendation in one to two sentences

The paper is well written and rather easy to follow. There are a few additional clarifications that could be added, which would further improve readability. As the method is only compared to "brute force" approaches, it is not entirely clear how it compares to other methods.

— *Gabriela Hug*

II. REVIEW #158B

A. Paper summary

This paper tackles the DC-SCOPF problem by performing 10 Kron reductions on identified areas of a network. To keep the formulation exact, coupling constraints are used to correct boundary injections. The paper results provide a very nice case study regarding the effectiveness of the proposed innovation.

B. Comments for authors

The innovation proposed in this paper is very compelling. By Kron reducing at boundary nodes, you effectively decouple the admittance matrices and "sparsify" the resulting PTDF matrices (by making them into blocks). The price you pay, though, is coupling constraints (other papers in the literature look at similar effects, e.g., Implementation of a Implementation of a Large-Scale Optimal Power Flow Solver Based on Semidefinite Programming, where clique merging is used to limit the number of coupling constraints). My three primary critiques follow. First, the decomposition method is combined with lazy constraint generation, so it's hard to compare the success of the method against $\mathbf{B} - \theta$ (to my knowledge, $\mathbf{B} - \theta$ formulation didn't use lazy constraint methods). Second, I am very surprised at how poorly the $\mathbf{B} - \theta$ method performed; I am curious if the implementation was optimal (e.g., sparsity was exploited, I assume?). Finally, authors didn't discuss how reduction areas were selected; I suspect this would heavily influence the method's success.

- "A Sparsification Method for Security-Constrained Optimal Power Flow" −> This title is good, but it could be improved. The authors use Kron + coupling to decompose the network into connected blocks. The paper strikes a balances between $\mathbf{B} - \theta$ and full PTDF. I feel the title could be more reflective of this.

- ”Although solving SCOPF with the PTDF is much faster than with the $\mathbf{B}-\theta$ model, the PTDF matrix is very dense in real-world systems, resulting in slow computational performance.” −> This sentence seems self-contradictory. The $\mathbf{B}-\theta$ formulation is a sparse LP, solvable in hundreds of miliseconds for even very large networks. Due to matrix density and elements' numerical ranges, the PTDF approach is often not scalable (hence, this paper).
- This might be semantics, but I do not see how (1) is a ”security constrained” formulation, since the contingencies are all penalized (i.e., if the base case is feasible, then all contingencies are feasible too).
- (3) is not stated clearly – what are c_1 and c_2?
- Fig 1 is not very legible.
- ”Fig. IV shows the nonzeros of the equality constraints” −> is this a typo? I am surprised at how poorly the $\mathbf{B}-\theta$ method performed in the test results. Two questions: (1) were the admittance matrices passed as true sparse matrices to the Gurobi solver, and (2), were the contingency admittance matrices re-built completely, or were corrections used? (I.e., B and B^c are very similar matrices, you just need a smaller perturbation of B to get B^c).
- Test results, otherwise, are very good.

C. Summarize your recommendation in one to two sentences

This paper proposes a nice innovation that makes large-scale SCOPF problem more scalable. The paper could be slightly improved by adding lazy constraint generation to the $\mathbf{B}-\theta$ approach and clarifying some implementation details (e.g., how the areas were selected). Overall, the paper is nice contribution to the PowerUp conference.

— Anonymous reviewer

III. Review #158C

A. Paper summary

The paper proposes a sparsification method to accelerate the solution of large-scale security-constrained optimal power flow (SC-OPF) problems. The proposed method is a Kron reduction-based decomposition method, built upon the sensitivity factor-based SCOPF models. Extensive simulation results on large-scale test systems show 3-7 speedup compared to baseline sensitivity factor-based formulation.

B. Comments for authors

The paper proposes an effective sparsification method for SC-OPF based on Kron reduction, decomposition, and lazy constraints. The effectiveness of the method is demonstrated through extensive computational experiments.

While there is evident computational advantage, the novelty of the work is not very clear to me. It is mentioned that one of the contributions is the development of a decomposition method for SC-OPF problem. However, as the authors have mentioned, similar decomposition idea appears in [18] and [19], it would strengthen the paper by highlighting what is novel compared to these existing works.

It is mentioned that the power balance equation (6) is equivalent to the actual system power balance equation if the consistency constraint is imposed after (8). It is not very clear in what sense they are equivalent. The DC power flow model has rotational symmetry so when no global reference bus is chosen, the phase angles are not uniquely determined in each area, and they can be inconsistent across different areas. This is different from an unreduced system model with one reference bus. The theoretical foundation of this being an ”exact” method, as the title suggests, is based on a reference to an earlier paper. A more specific pointer to a proposition or at least section of the reference would be much better.

There are some minor issue that are worth addressing:

1) The B matrix in (2) is singular so the inverse should be replaced by pseudoinverse. The power system graph modeling is repeated in Section III-A when they are introduced in II-A first.
2) The terms ”Kron reduction” and ”Gaussian elimination” are both used, the authors should pick one.
3) (8b) is referred to as the third equation when there are only two. In section III-D, the reference to the local susceptance matrix B^a is likely wrong. (9c) is an irrelevant equation after the sentence.
4) The expression ”... the PTDF matrix is a reference bus dependence” should be revised.
5) sustenance is a typo that appears a couple of times at the end of page 4 left column.

C. Summarize your recommendation in one to two sentences

The paper presents an effective sparsification method for SCOPF based on decomposition, while the presentation quality and the novelty claim should be improved.

— Bai Cui

IV. Brief response to reviewers (optional)

The authors express gratitude to the reviewers for their constructive feedback and valuable comments. We revised the paper and incorporated most of the reviewers' comments. A major comment from the reviewers is the poor computation speed of the $\mathbf{B}-\theta$ model. The $\mathbf{B}-\theta$ model performs very well, even better than the PTDF and decomposed PTDF models in the base OPF. However, the disadvantage of the $\mathbf{B}-\theta$ model is that when adding a new contingency, we must add full OPF constraints, which can reduce computational speed when considering a large number of contingencies. It's worth noting that there are several sophisticated methods and techniques to enhance the $\mathbf{B}-\theta$ model's performance that we did not consider, as they are out of scope for this paper. Nonetheless, we investigated direct methods, including lazy constraints and Bender decomposition, and found that solving the problem directly by providing the sparse formulation to a commercial solver (Gurobi) is the fastest approach. The other edits are as follows. First, we explicitly explained the novelty of the work proposed in this paper compared to the two references [18] and [19] that inspired this research direction. Second, we corrected all the typos and wrong figure references mentioned by the reviewers. Third, we clarified any ambiguity highlighted by the reviewers, including the definition of boundary buses, the singularity of the susceptance matrix, the definition of the contingency line notation, and the dependency of the PTDF matrix on the selection of the reference bus.

V. Brief summary of changes made to the final paper

Minor changes were made to address typos and improve notational clarity. Also, language was changed in certain places to make the exposition more clear for the reader.